High Solidity, Low Tip-Speed Rotors for Reduced eVTOL Tonal Noise

Farhan Gandhi Redfern Chair Professor
Justin Pepe MEng Student
Brendan Smith PhD Student

Center for Mobility with Vertical Lift (MOVE)
Rensselaer Polytechnic Institute, Troy, New York

ABSTRACT

This paper reports on a computational study conducted on an 8 ft diameter, fixed-pitch eVTOL rotor to examine the potential of using increased solidity and reduced tip speed to reduce the radiated acoustic signature. The study is conducted for the rotor operating in hover and in vertical climb, and at disk loadings between 6–12 lb/ft^2. Relative to a "nominal" rotor of solidity σ=0.0646 (with N=2 blades and a root chord, c=15.82 cm), two 3σ rotors (the 3σ3 rotor with N=3 and root chord of 2c, and the 3σ5 rotor with N=5 and root chord of 1.2c) operating at reduced tip speed are considered, as is a single 5σ rotor (with N=5 and root chord of 2c) operating at a further reduced tip speed. The high solidity, low tip-speed rotors showed significant reductions in in-plane noise, both in hover as well as vertical climb, and over the range of disk loadings considered. The noise reductions observed with the 3σ5 rotor were significantly greater than those obtained by the 3σ3 rotor (operating at the same tip speed), and very similar to those of the 5σ rotor (operating at a lower tip speed). But the rotor torque and power penalty for the 3σ5 rotor was considerably lower than that for the 5σ rotor. Overall, a high solidity in the range of 0.2 for eVTOL rotors is quite advantageous, but further increase to around 0.3 appears acoustically unnecessary while being aerodynamically detrimental. At a solidity of 3σ, going from 3 wider chord blades to 5 narrower chord blades was hugely influential for in-plane noise reduction. Of the configurations studied, the best (the 3σ5 rotor) showed 16–24 dB reductions in in-plane noise in hover, reducing to 14.5–20 dB at 5/ms climb rate, and 12.5–16 dB at 10 m/s climb rate, with larger reductions seen at lower disk loadings. Relative to the solidity-σ rotor, the 3σ rotors had a torque penalty of 41–44%, and power penalties ranging from 1.5–5% in hover, increasing to 7.5–10% at 10 m/s climb rate.

INTRODUCTION

The last few years have seen a tremendous interest in, and directed effort toward, the development of large eVTOL aircraft to support the Urban Air Mobility (UAM) vision. For the realization of this vision, where large eVTOL aircraft will ubiquitously ferry people, cargo, and packages across the urban and suburban landscape, it is critical that these aircraft have low noise signature for public acceptance. Accordingly, several studies have been conducted in recent years focusing both on specific eVTOL configurations, as well as a more general understanding of the effects of rotor-body, rotor-rotor, rotor-wing, rotor-rotor-ground interactions, and relative rotor phasing on eVTOL acoustics (e.g., Refs. 1–9).

Relative to conventional helicopters, eVTOL rotors have come to have certain distinguishing characteristics that are highly relevant from an acoustics perspective. For one, eVTOL rotors tend to operate at lower tip Mach numbers to minimize noise. Additionally, for footprint considerations and the fact that on many configurations they also double up as propellers, eVTOL rotors tend to be smaller, thus operating at significantly higher disk loading (than conventional helicopters) in the lifting-rotor mode. This is feasible on eVTOLs when hover and rotor-borne lift generation is limited in duration and the cruise segment relies on wing-borne lift. It should be noted that high rotor disk loading and simultaneously low operating tip Mach numbers generally require high rotor pitch setting as well as *high rotor solidity*. From Fig. 1 it is evident that the solidity on the Joby S4 rotors

Fig. 1: High-solidity rotors on the Joby S4

Presented at the Vertical Flight Society's 78th Annual Forum & Technology Display, Ft. Worth, TX, USA, May 10-12, 2022.

is much higher than typically used on conventional helicopters.

In this paper we seek to comprehensively investigate the acoustic characteristics of low tip Mach number, high-solidity, large UAM-scale eVTOL rotors. Over disk loading and tip Mach number ranges of interest for UAM operation, variation in rotor solidity is examined. Both increases in blade chord as well as number of blades are considered to increase rotor solidity, and results are compared. The study considers operation in hover as well as vertical climb, and tradeoffs in aerodynamic performance are examined.

ANALYSIS

The present study focuses on noise radiated by a single eVTOL rotor in hover and vertical climb conditions. The rotor aerodynamic loads are generated using the Rensselaer Multicopter Analysis Code (RMAC, Ref. 10), a comprehensive analysis as well as flight simulation code which uses blade element theory, coupled with the Peters-He finite state wake model for individual rotor load calculation. The blade loads are then provided as inputs to the acoustic propagation code PSU-WOPWOP (Ref. 11) along with the rotor geometries to calculate the acoustic pressure time histories at selected observer locations.

The acoustic pressure time histories are used to calculate the Sound Pressure Level (SPL) in dB over a desired frequency range, as well as the integrated Overall Sound Pressure Level (OASPL, also in dB) at the selected observer locations. RMAC also provides calculations of the integrated rotor thrust, torque, and power, with breakup of induced and profile components which are used for comparisons of rotor aerodynamic performance.

Since only hover and vertical climb conditions are considered in this study, there is no azimuthal variation in the noise radiated by the rotor. However, the radiated noise varies with elevation angle so an observer grid is arranged as a quarter circle at a distance of 15 rotor radii from the rotor hub in 10° increments in elevation angle, as shown in Fig. 2. At each observer the acoustic pressure time history, SPL spectrum, and OASPL are calculated for all the rotors in hover and climb. The noise sources are further broken up into thickness noise, loading noise, and overall noise allowing for a comparison of how these sources change with elevation angle as well as rotor geometry and operating condition.

RESULTS

The study considers an 8ft diameter rotor with 12% root cutout, whose blades have a –12 deg linear twist variation over the span, and a linear taper variation with a root to tip chord ratio of 4:3. The airfoil sections at the root and tip of the blade are the NACA 2412 and the Clark-Y, respectively, with a linear interpolation used in between. The nominal rotor solidity (σ) is 0.0646, similar to Ref. 12. With two blades (N=2), this results in a nominal root chord, c, of 15.82 cm. Rotors with three times the solidity (3σ rotors) and five times the solidity (5σ rotors) are also examined in this study. The higher solidity rotors have the same 12% root cutout, –12 deg linear twist, 4:3 linear taper, and airfoil distribution, as described above. Two different 3σ rotors are considered, the first with N=3, and root chord increased to 2c, and the second with N=5 and a root chord of 1.2c. The 5σ rotor has five blades (N=5) and a root chord of 2c. All of these different solidity rotors are represented schematically in Fig. 3. The study also considers the rotors at three different values of disk loading: 6 lb/ft^2, 9 lb/ft^2, and 12 lb/ft^2. While the lower value of disk loading would likely be more representative of multi-copters carrying large packages or cargo, the higher value of disk loading would be more typical of larger passenger carrying eVTOL aircraft.

6 lb/ft^2 Disk Loading in Hover

For a 6 lb/ft^2 disk loading in hover, Fig. 4 shows the variation in rotor tip Mach number, versus rotor root pitch, for different values of rotor solidity. Clearly, for any given solidity, the specified disk loading can be achieved by setting the rotor at a low root pitch and operating at a high tip Mach number, or conversely, by setting the rotor at a higher root pitch and operating at low tip Mach number. On conventional helicopters with fixed-RPM (variable pitch) rotors, the pitch is not set too high in order to preserve stall margin. On variable-RPM rotors, on the other hand, requirement for thrust increment can be met by speeding up the rotors. In that case, the rotor pitch can be set higher to allow for a lower nominal RPM, which is generally beneficial for acoustics. From Fig. 4, the blade root pitch is selected to be 21.5 deg (corresponding to a 9.5 deg pitch setting at the tip) for all values of solidity. Thus, as the rotor solidity increases, the hover tip Mach number decreases from 0.4327 for solidity σ, to 0.3087 for solidity 3σ, (for both the N=3, c= 2, as well as the N=5, c=1.2 cases), and further to 0.2744 for solidity 5σ.

In hover the propagated noise levels are independent of azimuth but do depend on elevation angle. For each of the four rotors in Fig. 3, the acoustic pressure time histories are calculated at observers placed at a distance of 15R from the rotor hub at 10 deg increments in elevation angle, ranging from 0 deg (in-plane) to 90 deg (directly below the rotor), as indicated in the Analysis section. Figure 5 shows a comparison of the total overall sound pressure level, as a function of elevation angle, for each of the four rotors. At high elevation angles and directly below the rotor, the propagated noise is observed to be similar, across the four configurations considered. For the nominal rotor (solidity σ, chord c, N=2), the noise does not show significant reduction at lower elevation angles. However, for the 3σ and 5σ rotors, the noise reduces considerably as elevation angle decreases, with the total OASPLs being lowest in the plane of the rotor (0 deg elevation). Compared to the nominal (solidity σ) rotor, the in-plane noise is seen to be 7 dB lower for the 3-bladed, 3σ rotor, and 24 dB lower for the 5-bladed (3σ and 5σ) rotors. The 3-bladed 3σ rotor with the 7 dB in-plane noise reduction has both a higher number of blades than the nominal rotor (N=3 compared to N=2), as well as a lower tip Mach number (0.3087 compared to 0.4327). The 5-bladed 3σ rotor has the

same tip Mach number as the 3-bladed 3σ rotor but shows an additional 17 dB reduction in in-plane noise. Clearly, when operating at 3σ solidity and a correspondingly reduced tip Mach number (0.3087), substantial reductions in in-plane noise are achieved with an increase of number of blades. The 5-bladed 3σ rotor and the 5σ rotor (which also has 5 blades, but each with a wider chord) operate at different tip Mach numbers (0.3087, compared to 0.2744) but have similar levels of in-plane noise. This suggests that with a larger number of blades (N=5) and an already reduced tip Mach number (of around 0.3), further reduction in tip Mach number (requiring an increase in blade chord) may not yield additional noise benefits.

Figure 6 provides a decomposition of the noise into thickness and loading components for each of the rotors discussed above. The thickness noise, as expected, is always maximum in-plane (0 deg elevation) and shows reduction with increase in blade solidity. By comparing Figs. 6b and 6c (both 3σ rotors) to Fig. 6a (the nominal solidity σ rotor) it can be observed that the increase in number of blades (from 3 to 5) seems to have a greater effect on in-plane thickness noise reduction than reduction in tip Mach number (from 0.4327 for the nominal rotor to 0.3087 for the two 3σ rotors). The loading noise is highest directly below the rotor and at high elevation angles, and comparable for all rotors. It shows a reduction with elevation angle and is minimum in-plane (0 deg elevation). While this reduction is small (of the order of 4 dB) for the nominal rotor, the 3σ and 5σ rotors show much larger reductions in loading noise in the plane of the rotor (of the order of 15–30 dB). As with the thickness noise, the increase in number of blades (from 3 to 5) seems to have a greater effect in reducing the in-plane loading noise than reduction in tip Mach number.

For the four rotor configurations discussed above, Figs. 7–10, show the acoustic pressure time histories (over one rotor revolution) at an in-plane observer situated 15R from the rotor hub, and the corresponding sound pressure level frequency spectra. For the nominal rotor (N=2 and solidity σ), Fig. 7a shows two pulses in the acoustic pressure time history corresponding to individual blade passage. As expected, in Fig. 8a three pulses are observed for the 3-bladed rotor, and in Figs. 9a and 10a, five pulses are observed when N=5. In hover, the operational speeds for the nominal rotor, the 3σ rotors, and the 5σ rotor are 1162.56 RPM, 829.27 RPM and 737.14 RPM, respectively. The blade passage frequencies (corresponding to the first peaks on Figs. 7b–10b) are, respectively, 38.75 Hz for the nominal rotor, 41.46 Hz for the 3σ, N=3 rotor, 69.11 Hz for the 3σ, N=5 rotor, and 61.43 Hz for the 5σ, N=5 rotor. It is noteworthy that for the higher solidity (3σ and 5σ) rotors, the higher number of blades and lower tip Mach numbers not only decreases the peak-to-peak variation in the acoustic pressure signals considerably (compare the y-axis ranges on the acoustic pressure time histories in Figs. 7a–10a), but also reduces the higher harmonic content (compare the sound pressure level frequency spectra in Figs. 7b–10b).

While it is clear from the above that high-solidity rotors, with a larger number of blades and operating at lower tip Mach numbers result in a reduction in tonal noise in hover, the rotor aerodynamic performance must also be considered. The rotor torque and power are calculated for each of the rotors considered and reported in Table 1. It is observed that the overall rotor power requirements show only a modest change (with the power increment for the 3σ rotors less than 1.5%, and that for the 5σ rotor less than 8%, relative to the nominal). The induced power requirements, of course, are most heavily dependent on the disk loading which is the same in all cases (6 lb/ft^2). The profile power requirement does not increase much, either, because the increase in solidity is compensated by the reduction in operational rotor RPM. The torque requirements, however, are seen to increase considerably, by 42.11% for the 3σ rotor and 69.83% for the 5σ rotor. Since motor sizing is based on the rotor torque requirements, the high-solidity rotors would require bigger (and heavier) motors.

9 lb/ft^2 Disk Loading in Hover

Since the root pitch of the rotor was already set high at 21.5 deg, it is not increased any further and the increase in disk loading to 9 lb/ft^2 is achieved by increasing the rotor speed. Table 2 lists the rotor speed (and the tip Mach number) for the σ, 3σ and 5σ cases corresponding to the increased 9 lb/ft^2 disk loading. Similar to Fig. 5 for the 6 lb/ft^2 disk loading, Fig. 11 shows a comparison of the total overall sound pressure level, as a function of elevation angle, for each of the four cases in Fig. 3. In general, the noise levels in Fig. 11 at 9 lb/ft^2 are all higher, as expected. Similar to Fig. 5, change in solidity has no effect on the noise below the rotor and at very high elevation angles, but the higher solidity 3σ and 5σ rotors with higher number of blades (N=3 or 5) are again quieter than the nominal rotor (with solidity σ and N=2) in-plane, and at low elevation angles. Compared to the nominal rotor, the in-plane noise level for the 3-bladed 3σ rotor is 5.5 dB lower, and the levels for the 5-bladed 3σ rotor and 5σ rotor are 19 dB lower.

At 9 lb/ft^2 in hover, the rotor torque and power requirements are also reported in Table 2. As was the case with the 6 lb/ft^2 disk loading in Table 1, the higher solidity rotors require modest increases in power of less than 3% for the 3σ rotors and around 8% for the 5σ rotor, relative to the nominal. The increases in torque requirement of 42.71% for the 3σ rotors and 69.29% for the 5σ rotor are remarkably similar to the increases previously observed at 6 lb/ft^2 disk loading.

12 lb/ft^2 Disk Loading in Hover

Increase in disk loading to 12 lb/ft^2 is achieved by further increasing the rotor speed (and operational tip Mach number), as reported in Table 3. Figure 12 shows a comparison of the total overall sound pressure level, as a function of elevation angle, for each of the four cases in Fig. 3. As expected, the noise levels in Fig. 12 at 12 lb/ft^2 are even higher than those at 9 lb/ft^2 in Fig. 11. Similar to Figs. 5 and 11, change in solidity has no effect on the noise below the rotor and at very

high elevation angles, but the higher solidity 3σ and 5σ rotors with higher number of blades (N=3 or 5) are again quieter than the nominal rotor in-plane, and at low elevation angles. Compared to the nominal rotor, the in-plane noise level for the 3-bladed, 3σ rotor is 4.5 dB lower, and the 5-bladed 3σ rotor and 5σ rotor are 16–16.5 dB quieter.

It should be noted that at 6 lb/ft^2 in Fig. 6, the loading noise was always maximum below the rotor and reduced as the elevation angle decreased (with greater reductions observed for high-solidity rotors with larger number of blades). In contrast, at 12 lb/ft^2 disk loading and a correspondingly higher operational tip Mach number, the nominal solidity-σ rotor showed an increase in loading noise at mid- and low-elevations (also observed to a lesser extent at 9 lb/ft^2). This increase in loading noise is the dominant contributor to the increase in total noise seen Fig. 12 at low elevation angles, and in-plane, for the nominal solidity-σ rotor operating at a 0.6 tip Mach number.

Similar to Figs. 7–10, Figs. 13 and 14 show acoustic pressure time histories and the corresponding sound pressure level frequency spectra at the in-plane observer 15R from the rotor hub at 12 lb/ft^2 disk loading, for the nominal rotor (N=2 and solidity σ) and the 3-bladed 3σ rotor. As noted in Table 3, the operational tip Mach number for the nominal rotor is 0.60, and that for the 3σ rotor is 0.44, at this higher disk loading. The acoustic waveform in Figs. 13a and 14a, and the frequency spectra in Figs. 13b and 14b have significantly greater higher harmonic content than that observed in Figs. 7 and 8 at the 6 lb/ft^2 disk loading.

At 12 lb/ft^2 in hover, the rotor torque and power requirements are also reported in Table 3. As with the lower disk loading cases in Tables 1 and 2, the higher solidity rotors require modest increases in power (under 5% for the 3σ rotors and under 7.5% for the 5σ rotor, relative to the nominal). The increases in torque requirement of 43.89% for the 3σ rotors and 67.64% for the 5σ rotor are also in a similar range to the increases previously observed at lower disk loadings.

6 lb/ft^2 Disk Loading in Vertical Climb

For a fixed-pitch rotor, the axial velocity experienced in climb would reduce angle of attack, and rotor speed has to be increased to maintain the required lift (Ref. 13). Table 4 shows the required rotor RPM values to maintain a 6 lb/ft^2 disk loading at a climb rate of 5 m/s and 10 m/s. Climb power for the σ, 3σ and 5σ rotors is shown in Fig. 15, with the values at 5 m/s and 10 m/s climb rates also reported in Table 4. Analogous to Fig. 5 in hover, Figs. 16 and 17 show a comparison of the total overall sound pressure level, as a function of elevation angle, for the σ, 3σ and 5σ rotors at climb rates of 5 m/s and 10 m/s, respectively. The in-plane noise for the nominal (solidity-σ) rotor increases from 79 dB in hover to 81.5 dB at 5 m/s climb rate and further to 84 dB at 10 m/s. As compared to maximum in-plane noise reductions of 24 dB in hover (Fig. 5), the reductions with high-solidity rotors with larger number of blades are limited to about 20 dB at 5 m/s climb rate (Fig. 16) and 16 dB at 10 m/s climb rate (Fig. 17).

From Table 4, the 3σ rotors show a power increase of 5.4% at 5 m/s climb rate and 9.5% at 10 m/s climb rate, relative to the nominal solidity-σ rotor. These power penalties are significantly greater than the less than 1.5% penalty in hover. Power penalties for the 5σ rotor are even greater – 9.52% at 5 m/s climb rate and 19.57% at 10 m/s climb rate (compared to a penalty of 7.66% in hover). At both climb speeds, the nearly 42% increase in torque for the 3σ rotor and the 66–68% increase in torque for the 5σ rotor are similar to the torque increases seen in hover over the nominal solidity-σ rotor.

9 lb/ft^2 Disk Loading in Vertical Climb

Table 5 shows the required rotor RPM values to maintain a 9 lb/ft^2 disk loading at a climb rate of 5 m/s and 10 m/s. Climb power for the σ, 3σ and 5σ rotors is shown in Fig. 18, with the values at 5 m/s and 10 m/s climb rates also reported in Table 5. Analogous to Fig. 11 in hover, Figs. 19 and 20 show a comparison of the total overall sound pressure level, as a function of elevation angle, for the σ, 3σ and 5σ rotors. The in-plane noise for the nominal (solidity-σ) rotor increases from 86 dB in hover to 88 dB at 5 m/s climb rate and further to 90.5 dB at 10 m/s. As compared to maximum in-plane noise reductions of 19 dB in hover (Fig. 11), the reductions with high-solidity rotors with larger number of blades are limited to about 17 dB at 5 m/s climb rate (Fig. 19) and 14 dB at 10 m/s climb rate (Fig. 20).

From Table 5, the 3σ rotors show a power increase of 4.2% at 5 m/s climb rate and 7.9% at 10 m/s climb rate, relative to the nominal solidity-σ rotor. These power penalties are again greater than the 2.64% penalty in hover. Power penalties for the 5σ rotor are 7.9% at 5 m/s climb rate and 16.8% at 10 m/s climb rate (compared to an 8.05% penalty in hover). At both climb speeds, the nearly 41% increase in torque for the 3σ rotor and the 66% increase in torque for the 5σ rotor are comparable to torque increases seen in hover over the nominal solidity-σ rotor.

12 lb/ft^2 Disk Loading in Vertical Climb

Table 6 shows the required rotor RPM values to maintain a 12 lb/ft^2 disk loading at a climb rate of 5 m/s and 10 m/s. Climb power for the σ, 3σ and 5σ rotors is shown in Fig. 21, with the values at 5 m/s and 10 m/s climb rates also reported in Table 6. Analogous to Fig. 12 in hover, Figs. 22 and 23 show a comparison of the total overall sound pressure level, as a function of elevation angle, for the σ, 3σ and 5σ rotors. The in-plane noise for the nominal (solidity-σ) rotor increases from 91.5 dB in hover to 93.5 dB at 5 m/s climb rate and further to 95.5 dB at 10 m/s. As compared to maximum in-plane noise reductions of 16.5 dB in hover (Fig. 12), the reductions with high-solidity rotors with larger number of blades are limited to about 14.5 dB at 5 m/s climb rate (Fig. 22) and 12.5 dB at 10 m/s climb rate (Fig. 23).

From Table 6, the 3σ rotors show a power increase of 4.1% at 5 m/s climb rate and 7.5% at 10 m/s climb rate, relative to the nominal solidity-σ rotor. In comparison, the power penalty was 4.65% in hover. Power penalties for the 5σ rotor are 10.7% at 5 m/s climb rate and 15.4% at 10 m/s climb rate (compared to an 7.38% penalty in hover). At both climb speeds, the nearly 41% increase in torque for the 3σ rotor and the 65–66% increase in torque for the 5σ rotor are generally similar to the torque increases seen in hover over the nominal solidity-σ rotor.

CONCLUSIONS

This paper reports on a computational study conducted on a single 8 ft diameter eVTOL rotor to examine the potential of using increased solidity and reduced tip speed to reduce the radiated acoustic signature (specifically the tonal noise). The study is conducted for the rotor operating in hover and in vertical climb conditions, and at three different values of disk loading (6 lb/ft^2, 9 lb/ft^2, and 12 lb/ft^2). Relative to a "nominal" rotor of solidity σ=0.0646 (with N=2 blades and a root chord, c=15.82 cm), two 3σ rotors (the 3σ3 rotor with N=3 and root chord of 2c, and the 3σ5 rotor with N=5 and root chord of 1.2c) operating at reduced tip speed are considered, as is a single 5σ rotor (with N=5 and root chord of 2c) operating at a further reduced tip speed. From the results obtained, the following key conclusions can be drawn:

1. In hover, the 3σ3 rotor showed 4.5–7 dB reductions in in-plane noise, relative to the nominal, but the two 5-bladed configurations (the 3σ5 and 5σ rotors) showed substantially greater reductions (16–24 dB). The noise reductions were greatest at the lowest disk loading (7 dB for 3σ3 rotor and 24 dB for the two 5-bladed configurations at 6 lb/ft^2) and least at the highest disk loading (4.5 dB for 3σ3 rotor and 16 dB for the two 5-bladed configurations at 12 lb/ft^2). Since the 3σ3 and 3σ5 rotors operate at the same reduced tip Mach number relative to the nominal solidity-σ rotor, it is clear that increase in number of blades from 3 to 5 (at a high solidity of 0.194) is significant for in-plane noise reduction. On the other hand, going from the 3σ5 to the 5σ configuration resulted in no further reduction in in-plane noise. In other words, if the rotor had 5-blades, increasing its solidity from 0.194 to 0.323, along with a corresponding reduction in tip Mach number, resulted in no further acoustic benefit.
2. The in-plane noise reductions with the use of the higher-solidity, lower tip-speed rotors are smaller in vertical climb than in hover, but they still remain very significant. For the 5-bladed configurations (3σ5 and 5σ rotors) in-plane noise reductions at 6 lb/ft^2 disk loading were 20 dB at 5 m/s climb rate and 16 dB at 10 m/s climb rate (relative to 24 dB in hover). At 9 lb/ft^2 disk loading the corresponding reductions were 17 dB at 5 m/s and 14 dB at 10 m/s (relative to 19 dB in hover), and at 12 lb/ft^2 disk loading reductions of 14.5 dB at 5 m/s and 12.5 dB at 10 m/s were observed (relative to 16–16.5 dB in hover),
3. The use of the higher-solidity rotors increases rotor torque requirement. 41–44% increases were observed for both 3σ rotors, and 65–70% increases were observed for the 5σ rotor, across variations operating condition (disk loading ranging from 6–12 lb/ft^2, and hover as well as vertical climb at 5 m/s and 10 m/s).
4. The use of the higher-solidity rotors also increases power requirement. Increases of 1.5–5% were observed for the 3σ rotors in hover, while the corresponding increases were in the range of 7.5–8% for the 5σ rotor. The power penalty at 10 m/s climb rate was observed to increase to 7.5–10% for the 3σ rotors and to 15–20% for the 3σ rotor.
5. Overall, the 5-bladed 3σ rotor (solidity of 0.194) was observed to be as quiet as the 5σ rotor, but had significantly lower torque and power penalties. It would appear, then, that a high solidity in the range of 0.2 for eVTOL rotors is quite advantageous, but further increase to around 0.3 appears acoustically unnecessary while being aerodynamically detrimental. At a solidity of 0.194, going from 3 wider chord blades to 5 narrower chord blades was hugely influential for in-plane noise reduction.

ACKNOWLEDGEMENTS

Support for this study was provided by Sikorsky Aircraft Corporation. Dr. Cal Sargent, Dr. Vineet Sahasrabudhe, and Mr. Jim Andrews of Sikorsky are gratefully acknowledged.

REFERENCES

1. Quackenbush, T., Wachspress, D., Moretti, L., Barwey, D., Lewis, R., and Brentner, K., "Aeroacoustic Modeling of an eVTOL Slowed Rotor Winged Compound Aircraft," 75th Annual Forum of the Vertical Flight Society, Philadelphia, PA, May 2019.
2. Wachspress, D., Yu, M., and Brentner, K., "Rotor/Airframe Aeroacoustic Prediction for eVTOL UAM Aircraft," 75th Annual Forum of the Vertical Flight Society, Philadelphia, PA, May 2019.
3. Jia, Z., and Lee, S., "Acoustic Analysis of Urban Air Mobility Quadrotor Aircraft," Vertical Flight Society's Transformative Vertical Flight Forum, San Jose, CA, Jan 21-23, 2020.
4. Alvarez, J. E., Schenk, A., Critchfield, T., Ning, A., "Rotor-on-Rotor Aeroacoustic Interactions of Multirotor in Hover," 76th Annual Forum of the Vertical Flight Society, Virtual, 2020.
5. Smith, B., Gandhi, F., and Niemiec, R., "A Comparison of Multicopter Noise Characteristics with Increasing Number of Rotors" 76th Annual Forum of the Vertical Flight Society, Virtual, 2020.
6. Smith, B., Gandhi, F., and Lyrintzis, A., *"An Assessment of Multicopter Noise in Edgewise Flight,"* Proceedings of the 77th Vertical Flight Society Annual Forum, Virtual, May 10–14, 2021.
7. Smith, B., Healy, R., Gandhi, F., and Lyrintzis, A., *"eVTOL Rotor Noise in Ground Effect,"* Proceedings of

the 77th Vertical Flight Society Annual Forum, Virtual, May 10–14, 2021.
8. Passe, B. and Baeder, J., "Computational Aeroacoustics of Different Propeller Configurations for eVTOL Applications," Vertical Flight Society's Autonomous VTOL Technical Meeting and Electric VTOL Symposium, Mesa, Arizona, Jan. 2019.
9. Zhang, J., Brentner, K., and Smith, E., "Prediction of the Aerodynamic and Acoustic Impact of Propeller-Wing Interference," Proceedings of the Vertical Flight Society's Aeromechanics for Advanced Vertical Flight Technical Meeting, San Jose, California, Jan 21-23, 2020.
10. Niemiec, R. and Gandhi, F., "Development and Validation of the Rensselaer Multicopter Analysis Code (RMAC): A Physics-Based Comprehensive Modeling Tool," 75th Annual Forum of the Vertical Flight Society, Philadelphia, PA, May 2019
11. Brentner, K., Bres, G. A., and Perez, G., "Maneuvering Rotorcraft Noise Prediction: A New Code for a New Problem," AHS Aerodynamics, Acoustics, and Test and Evaluation Technical Specialist Meeting, San Francisco, CA, Jan. 2002.
12. Johnson, W., "A Quiet Helicopter for Air Taxi Operations," VFS Aeromechanics for Advanced Vertical Flight Technical Meeting, San Jose, California, Jan. 2020.
13. McKay, M., Niemiec, R., and Gandhi, F., "Performance Comparison of Quadcopters with Variable-RPM and Variable-Pitch Rotors," *J. of the American Helicopter Society*, Vol. 64, No. 4, Oct 2019. https://doi.org/10.4050/JAHS.64.042006.

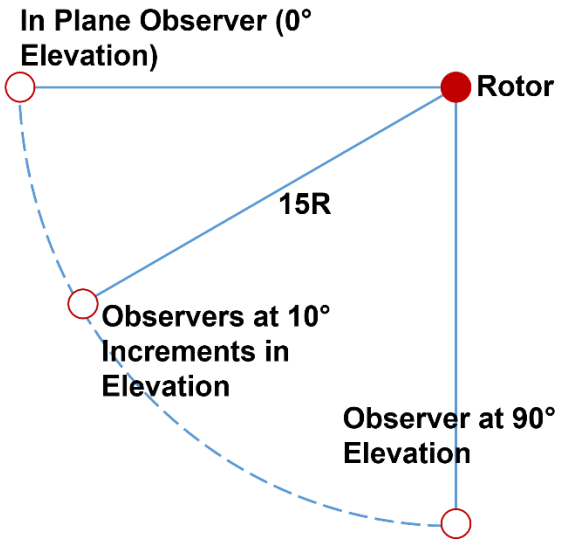

Figure 2 – Observer Grid Location

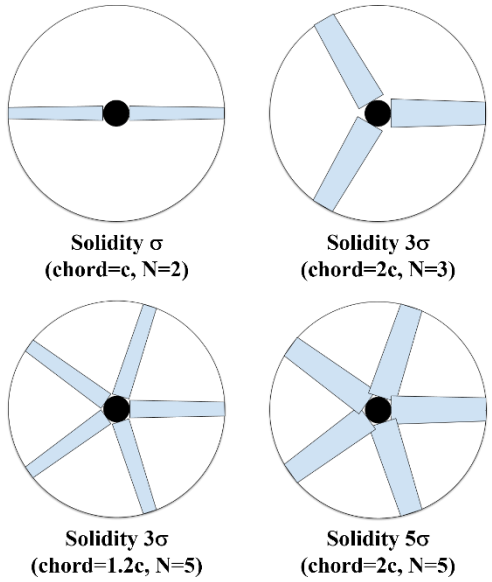

Figure 3 – Rotors of increasing solidity

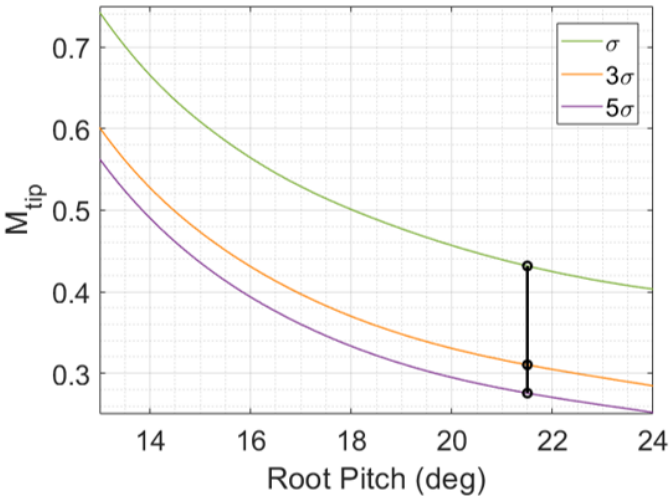

Figure 4 – Variation in rotor pitch and tip Mach number for 6 lb/ft^2 disk loading in hover

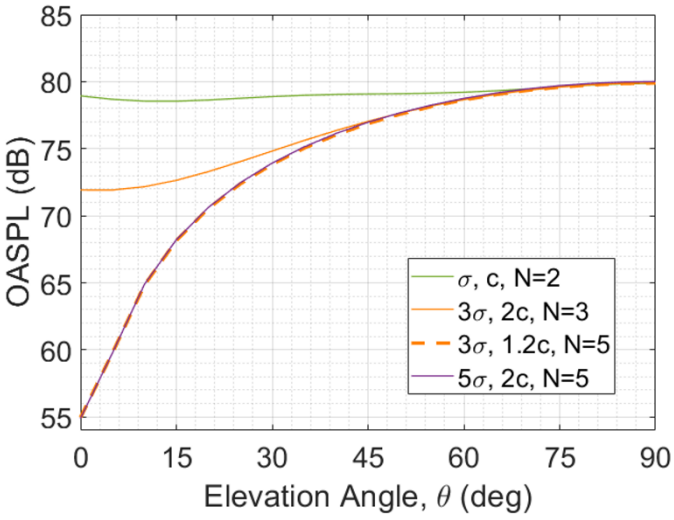

Figure 5 – Overall Sound Pressure Level (OASPL) across observer grid for 6 lb/ft^2 disk loading in hover

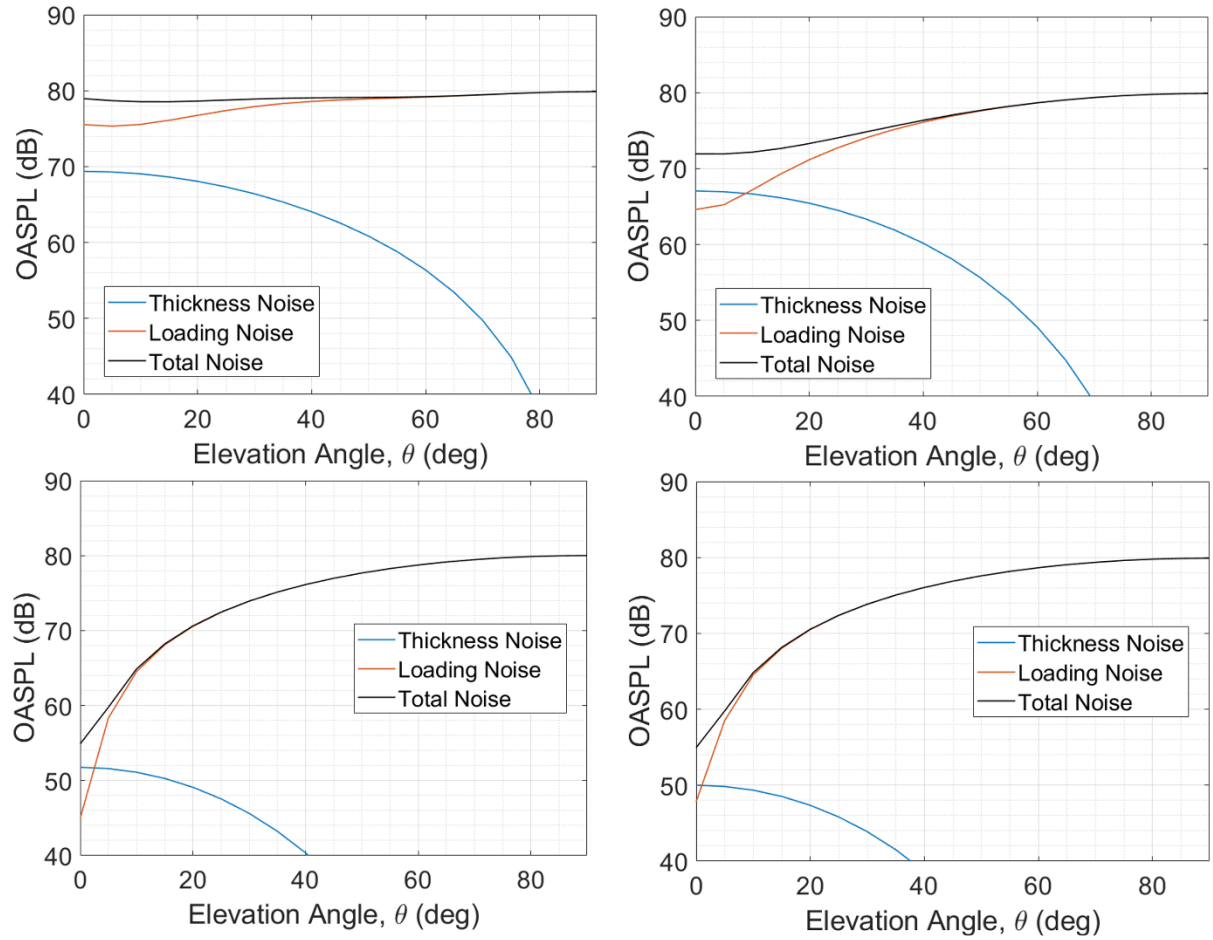

Figure 6 – Breakup of noise into thickness, loading, overall components for 6 lb/ft^2 rotors in hover with solidity of (a) Top Left: σ (b) Top Right: 3σ, N = 3 (c) Bottom Right: 3σ, N = 5 (d) Bottom Left: 5σ

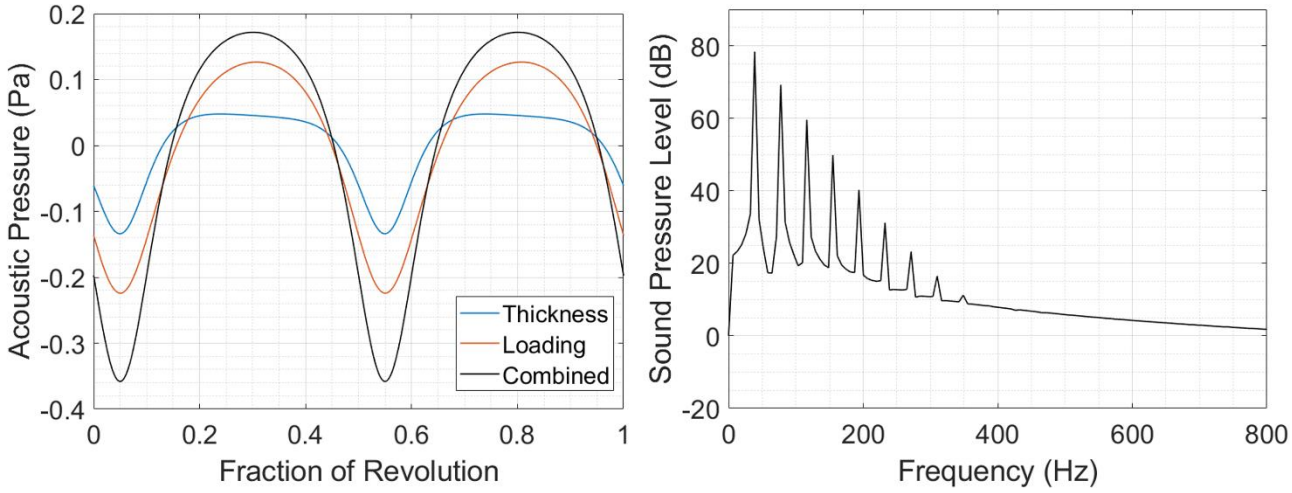

Figure 7 – 6 lb/ft^2 disk loading in hover, in plane observer, rotor solidity of σ (a) Left: Acoustic pressure time history (b) Right: SPL frequency spectrum

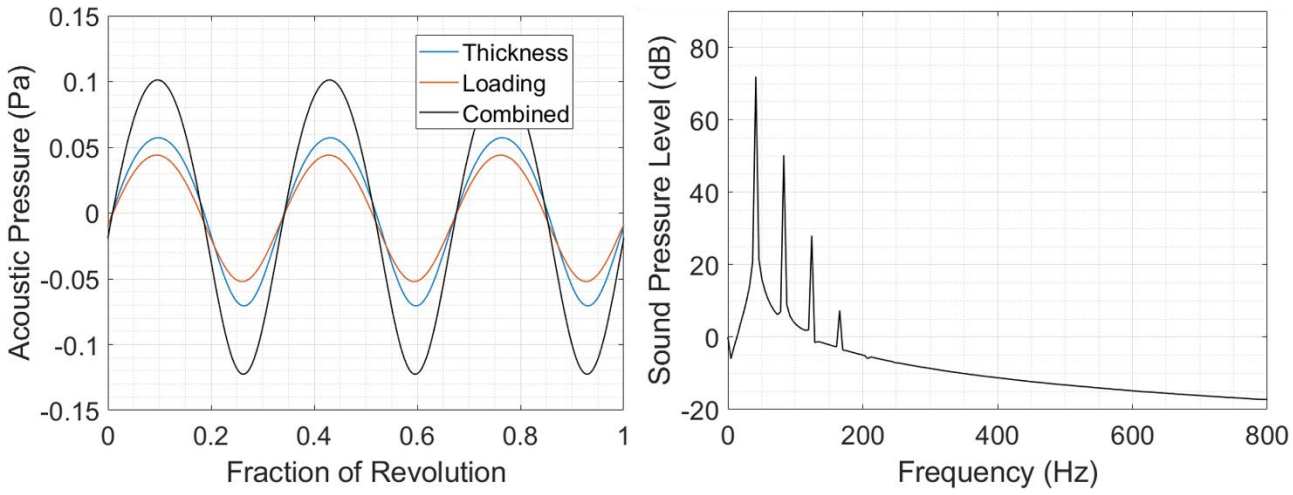

Figure 8 – 6 lb/ft^2 disk loading in hover, in plane observer, rotor solidity of 3σ, N = 3 (a) Left: Acoustic pressure time history (b) Right: SPL frequency spectrum

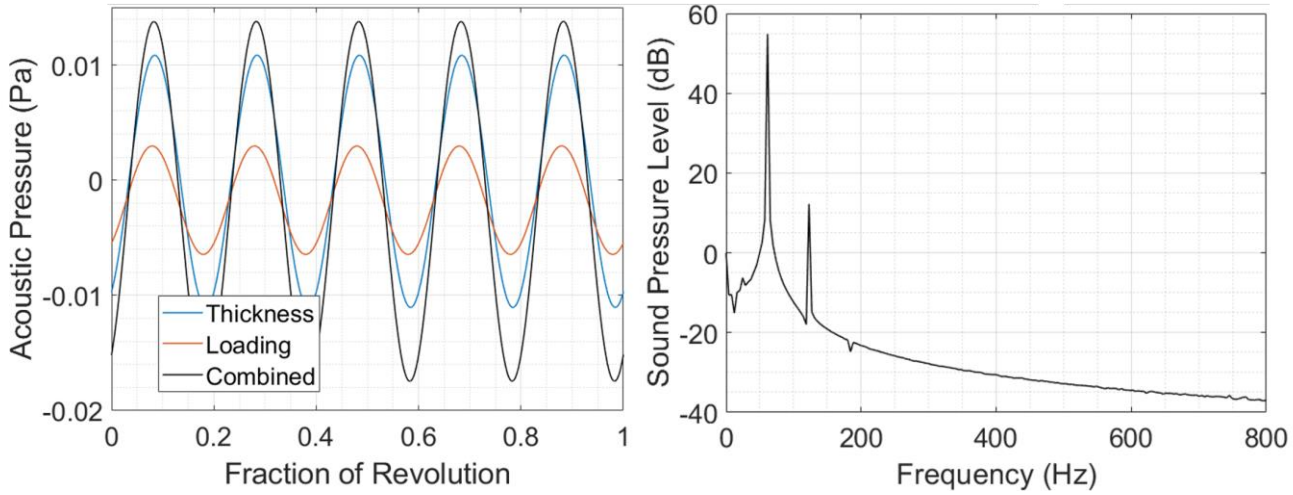

Figure 9 – 6 lb/ft^2 disk loading in hover, in plane observer, rotor solidity of 3σ, N = 5 (a) Left: Acoustic pressure time history (b) Right: SPL frequency spectrum

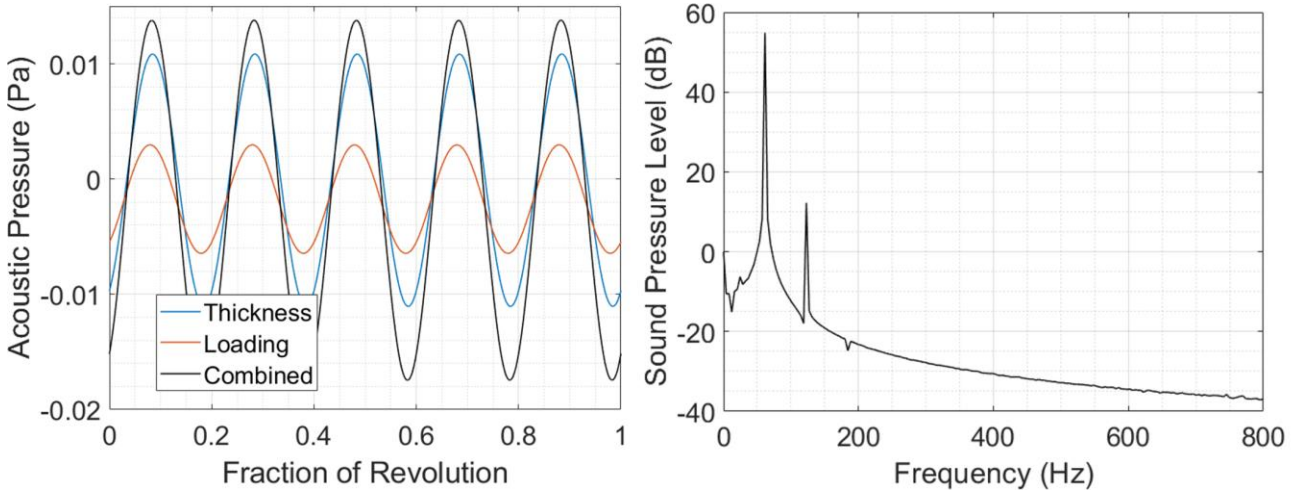

Figure 10 – 6 lb/ft^2 disk loading in hover, in plane observer, rotor solidity of 5σ (a) Left: Acoustic pressure time history (b) Right: SPL frequency spectrum

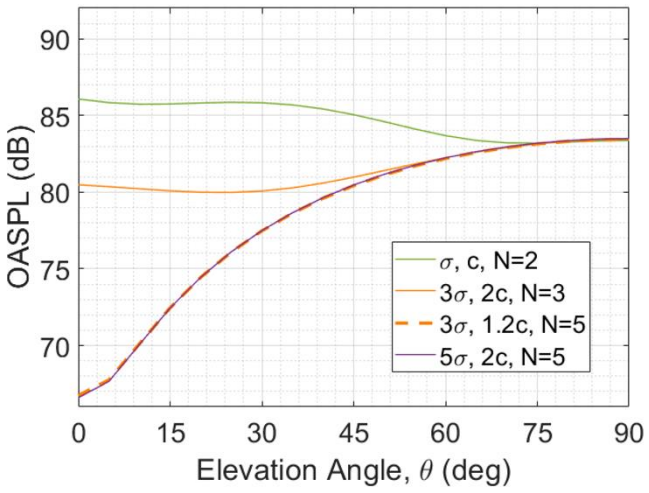

Figure 11 – Overall Sound Pressure Level (OASPL) across observer grid for 9 lb/ft^2 disk loading in hover

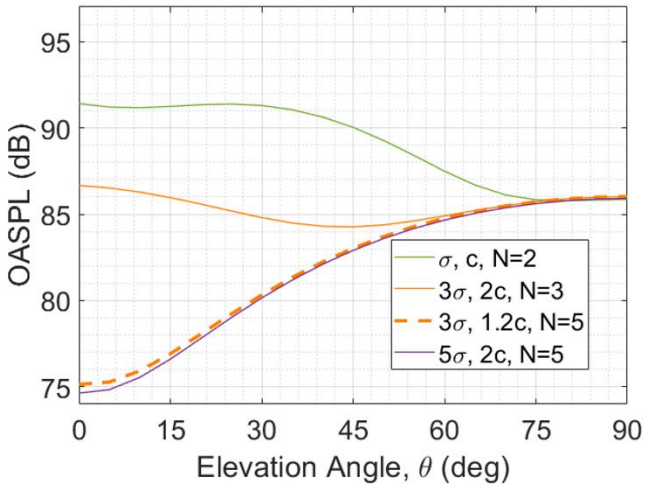

Figure 12 – Overall Sound Pressure Level (OASPL) across observer grid for 12 lb/ft^2 disk loading in hover

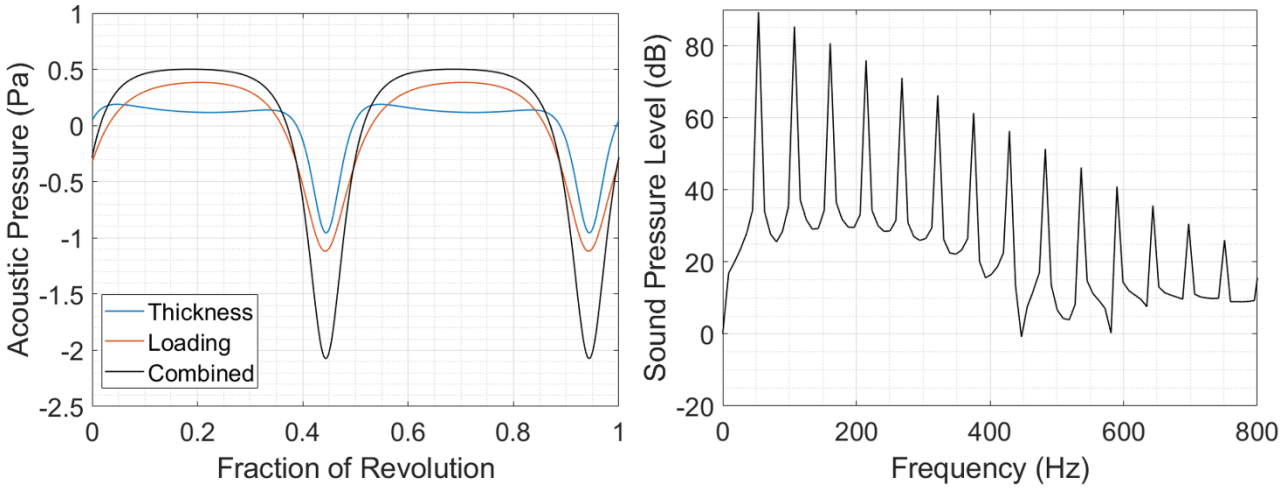

Figure 13 – 12 lb/ft^2 disk loading, in plane observer, rotor solidity of σ (a) Left: Acoustic pressure time history (b) Right: SPL frequency spectrum

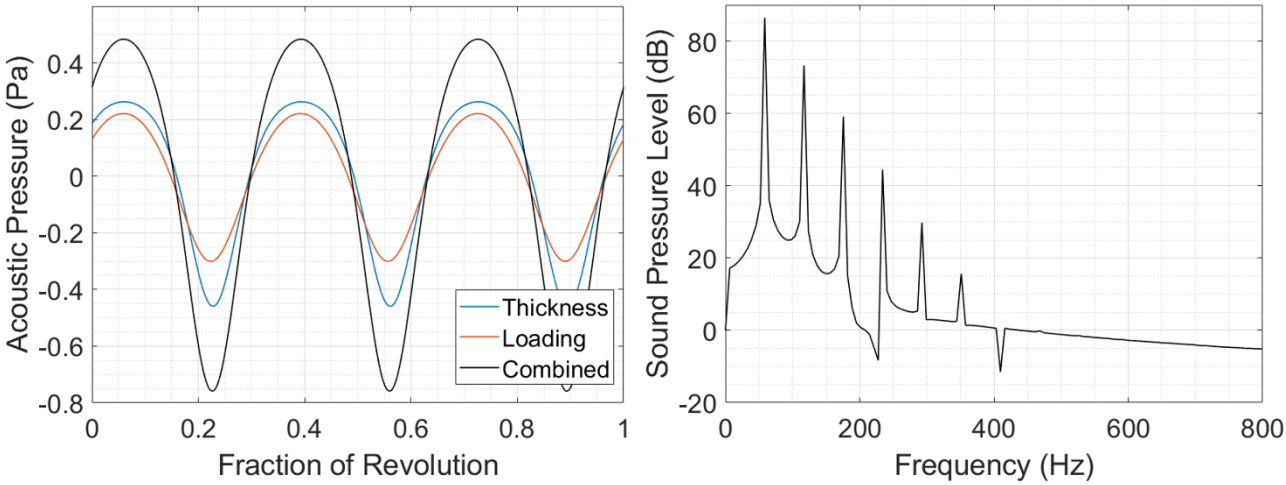

Figure 14 – 12 lb/ft^2 disk loading, in plane observer, rotor solidity of 3σ, N = 3 (a) Left: Acoustic pressure time history (b) Right: SPL frequency spectrum

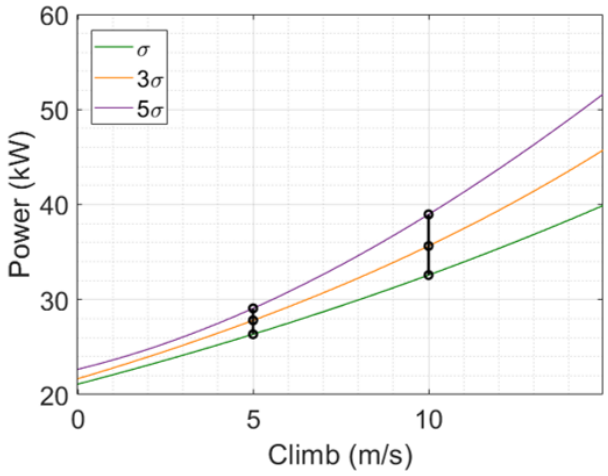

Figure 15 – 6 lb/ft^2 rotor power consumption for climb rates up to 15 m/s

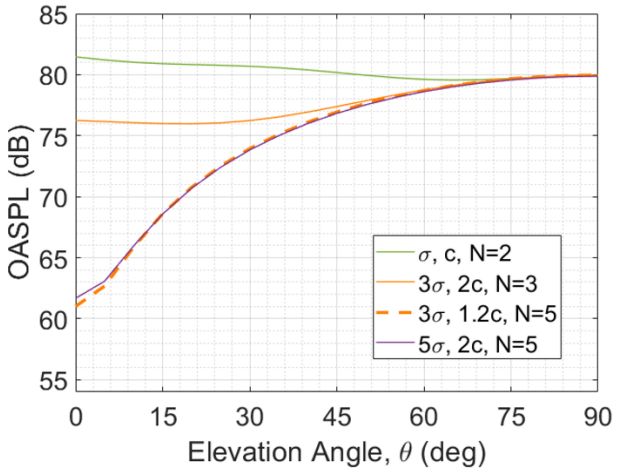

Figure 16 – Overall Sound Pressure Level (OASPL) across observer grid for 6 lb/ft^2 disk loading at 5 m/s axial climb

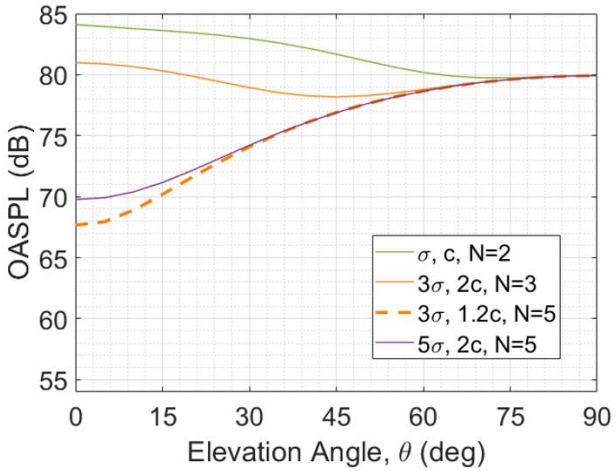

Figure 17 – Overall Sound Pressure Level (OASPL) across observer grid for 6 lb/ft^2 disk loading at 10 m/s axial climb

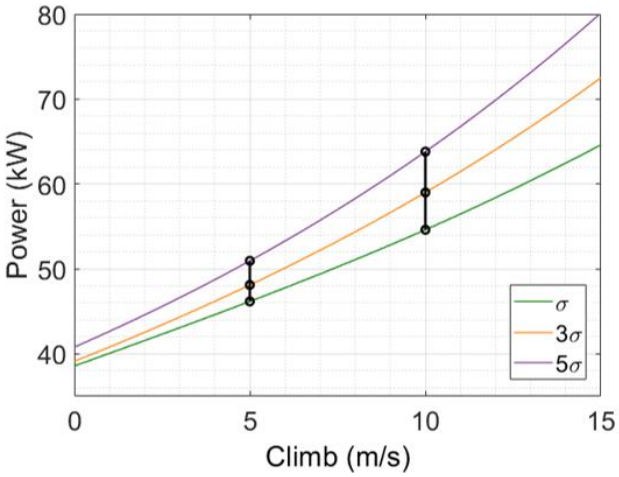

Figure 18 – 9 lb/ft^2 rotor power consumption for climb rates up to 15 m/s

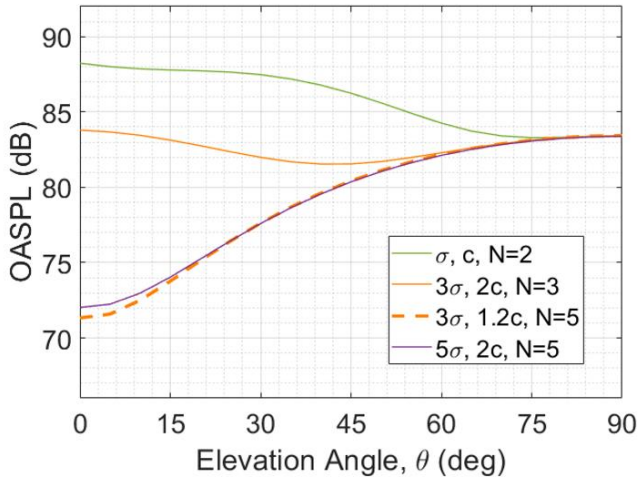

Figure 19 – Overall Sound Pressure Level (OASPL) across observer grid for 9 lb/ft^2 disk loading at 5 m/s axial climb

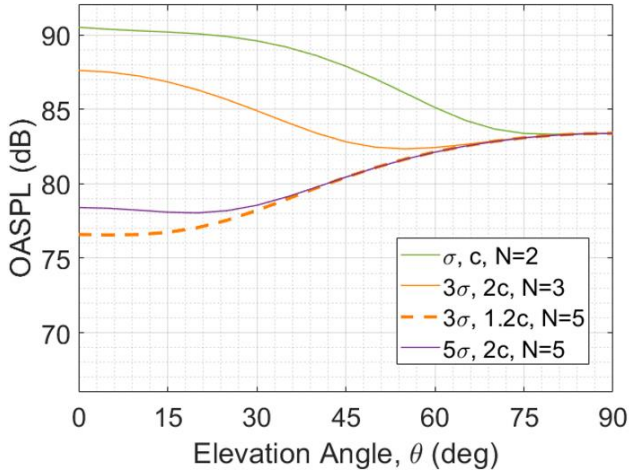

Figure 20 – Overall Sound Pressure Level (OASPL) across observer grid for 9 lb/ft^2 disk loading at 10 m/s axial climb

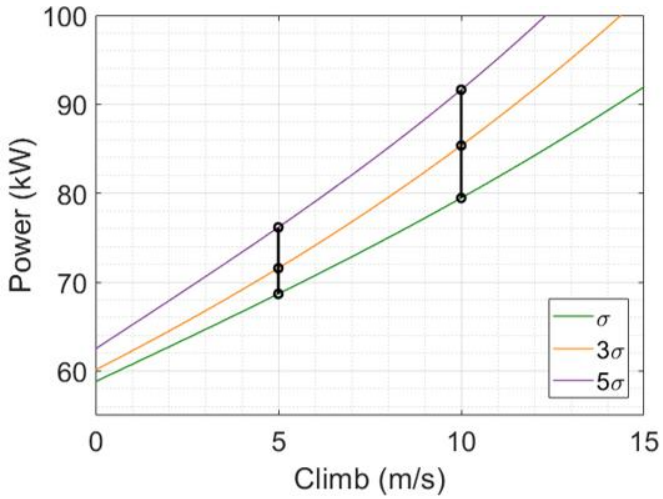

Figure 21 – 12 lb/ft^2 rotor power consumption for climb rates up to 15 m/s

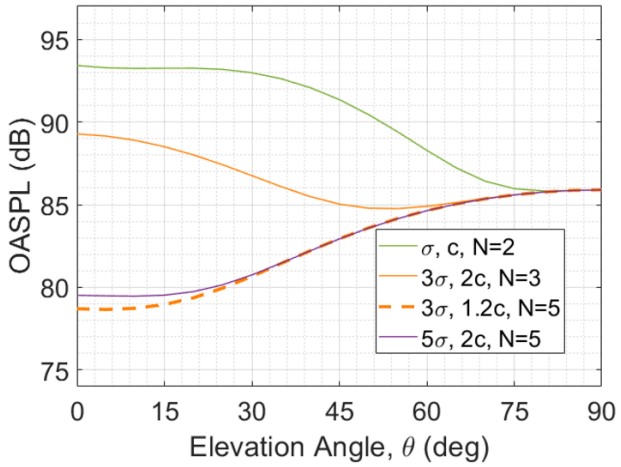

Figure 22 – Overall Sound Pressure Level (OASPL) across observer grid for 12 lb/ft^2 disk loading at 5 m/s axial climb

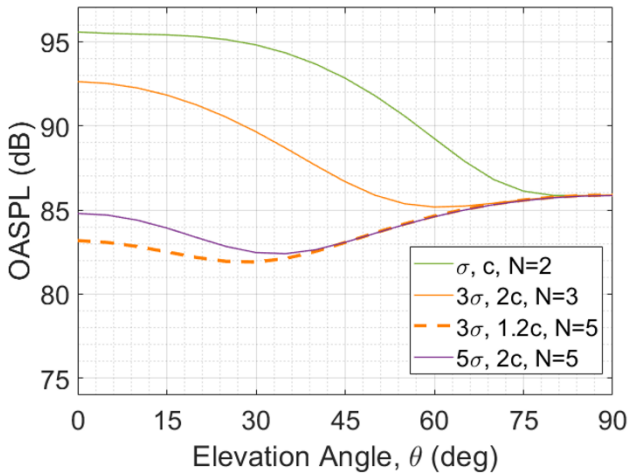

Figure 23 – Overall Sound Pressure Level (OASPL) across observer grid for 12 lb/ft^2 disk loading at 10 m/s axial climb

Table 1 – Performance of 6 lb/ft^2 rotors in hover

Solidity	RPM	M_tip	Blade Passage Freq (Hz)	Power (kW)	Torque (N-m)
σ	1162.56	0.4327	38.75	21.27	174.71
3σ	829.27	0.3087	41.46 (N=3) 69.11 (N=5)	21.56	248.28
5σ	737.14	0.2744	61.43	22.90	296.71

Table 2 – Performance of 9 lb/ft^2 rotors in hover

Solidity	RPM	M_tip	Blade Passage Freq (Hz)	Power (kW)	Torque (N-m)
σ	1408.55	0.5243	46.95	38.65	262.00
3σ	1013.32	0.3772	50.67 (N=3) 84.44 (N=5)	39.67	373.89
5σ	898.96	0.3346	74.91	41.76	443.55

Table 3 – Performance of 12 lb/ft^2 rotors in hover

Solidity	RPM	M_tip	Blade Passage Freq (Hz)	Power (kW)	Torque (N-m)
σ	1609.24	0.5990	53.64	58.93	349.68
3σ	1170.29	0.4356	58.51 (N=3) 97.54 (N=5)	61.67	503.17
5σ	1030.93	0.3837	85.90	63.28	586.21

Table 4 – Performance of 6 lb/ft^2 rotors in 5 and 10 m/s axial climb

Solidity	RPM	M_tip	Blade Passage Freq (Hz)	Power (kW)	Torque (N-m)
5 m/s climb rate					
σ	1244.09	0.4631	41.47	26.34	202.18
3σ	923.16	0.3436	46.16 (N=3) 76.93 (N=5)	27.76	287.12
5σ	831.03	0.3093	69.25	29.25	336.12
10 m/s climb rate					
σ	1343.35	0.5000	44.78	32.55	231.41
3σ	1040.10	0.3871	52.01 (N=3) 86.68 (N=5)	35.65	327.33
5σ	958.26	0.3567	76.85	38.92	387.87

Table 5 – Performance of 9 lb/ft^2 rotors in 5 and 10 m/s axial climb

Solidity	RPM	M_tip	Blade Passage Freq (Hz)	Power (kW)	Torque (N-m)
5 m/s climb rate					
σ	1488.15	0.5539	49.61	46.15	296.12
3σ	1099.84	0.4094	54.99 (N=3) 91.65 (N=5)	48.09	417.53
5σ	989.77	0.3684	82.48	50.86	490.69
10 m/s climb rate					
σ	1557.96	0.5837	52.60	54.65	330.69
3σ	1209.61	0.4502	60.48 (N=3) 100.8 (N=5)	58.98	465.61
5σ	1108.19	0.4125	93.35	63.83	550.03

Table 6 – Performance of 12 lb/ft^2 rotors in 5 and 10 m/s axial climb

Solidity	RPM	M_tip	Blade Passage Freq (Hz)	Power (kW)	Torque (N-m)
5 m/s climb rate					
σ	1685.85	0.6275	56.19	68.67	388.96
3σ	1247.90	0.4645	62.39 (N=3) 103.99 (N=5)	71.47	546.93
5σ	1124.47	0.4185	93.71	76.00	645.45
10 m/s climb rate					
σ	1770.41	0.6590	59.01	79.46	428.61
3σ	1353.57	0.5038	67.68 (N=3) 112.8 (N=5)	85.38	602.36
5σ	1235.44	0.4598	102.95	91.70	708.78